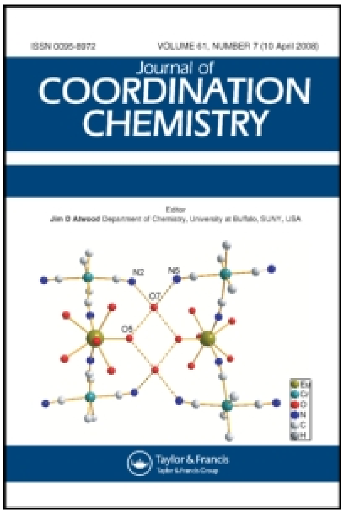

Journal of Coordination Chemistry
Publication details, including instructions for authors and subscription information:
http://www.informaworld.com/smpp/title~content=t713455674

Synthesis, characterization, and crystal structure determination of two copper(II) complexes: $[Cu(dm4bt)Cl_2(DMSO)]$ and $[\{Cu(dm4bt)(H_2O)(tpht)\} \cdot H_2O]_{<i>n</i>}$

Radhiya Al-Hashemi[a]; Nasser Safari[a]; Saeid Amani[b]; Vahid Amani[a]; Anita Abedi[c]; Hamid Reza Khavasi[a]; Seik Weng Ng[d]
[a] Department of Chemistry, Shahid Beheshti University, Tehran 1983963113, Iran [b] Department of Chemistry, Arak University, Arak 38156, Iran [c] Department of Chemistry, North Tehran Branch, Islamic Azad University, Tehran, Iran [d] Department of Chemistry, Malaya University, 50603 Kuala Lumpur, Malaysia

To cite this Article Al-Hashemi, Radhiya , Safari, Nasser , Amani, Saeid , Amani, Vahid , Abedi, Anita , Reza Khavasi, Hamid and Weng Ng, Seik(2010) 'Synthesis, characterization, and crystal structure determination of two copper(II) complexes: $[Cu(dm4bt)Cl_2(DMSO)]$ and $[\{Cu(dm4bt)(H_2O)(tpht)\} \cdot H_2O]_{<i>n</i>}$', Journal of Coordination Chemistry, 63: 18, 3207 — 3217, First published on: 11 August 2010 (iFirst)

To link to this Article: DOI: 10.1080/00958972.2010.509794

URL: http://dx.doi.org/10.1080/00958972.2010.509794

Journal of Coordination Chemistry
Vol. 63, No. 18, 20 September 2010, 3207–3217

Synthesis, characterization, and crystal structure determination of two copper(II) complexes: [Cu(dm4bt)Cl_2(DMSO)] and [{Cu(dm4bt)(H_2O)(tpht)} $\cdot$ H_2O]$_n$

RADHIYA AL-HASHEMI†, NASSER SAFARI*†, SAEID AMANI‡,
VAHID AMANI†, ANITA ABEDI§,
HAMID REZA KHAVASI† and SEIK WENG NG¶

†Department of Chemistry, Shahid Beheshti University,
G.C., Evin, Tehran 1983963113, Iran
‡Department of Chemistry, Arak University,
Dr Beheshti Avenue, Arak 38156, Iran
§Department of Chemistry, North Tehran Branch,
Islamic Azad University, Tehran, Iran
¶Department of Chemistry, Malaya University,
50603 Kuala Lumpur, Malaysia

(*Received 19 February 2010; in final form 21 May 2010*)

Copper complexes, [Cu(dm4bt)Cl_2(DMSO)] (**1**) and [{Cu(dm4bt)(H_2O)(tpht)} $\cdot$ H_2O]$_n$ (**2**) (dm4bt, 2,2′-dimethyl-4,4′-bithiazole; tpht, terephthalate), have been synthesized and their crystal structures were determined by X-ray crystallography. Complex **1** was prepared from a reaction of $CuCl_2 \cdot 2H_2O$ with dm4bt and terephthalic acid in a mixture of methanol, water, and DMSO. Complex **2** was prepared from a reaction of $CuCl_2 \cdot 2H_2O$ with dm4bt, terephthalic acid, and ethylene diamine in a mixture of methanol and water. The two complexes were characterized by IR, UV-Vis spectroscopy, and single-crystal structure. Complex **2** was also characterized by electron paramagnetic resonance spectra. Complex **1** is a monomer while **2** is a coordination polymer. This copper tpht polymer has a cis-configuration of tpht rings opposed to *zigzag* chains with *anti*-configuration usually reported in the literature.

Keywords: Copper; 2,2′-Dimethyl-4,4′-bithiazole; Dimethyl sulfoxide; Terephthalic acid; Crystal structure

1. Introduction

Metal coordination polymers containing dicarboxylates as organic spacer have fascinating architectures and advantageous properties, such as bulk magnetic behavior, photoluminescence, optical activity, catalysis, gas adsorption, high dimensionality and thermal stability [1–3].

Design and construction of polynuclear complexes or multi-dimensional coordination polymers with metal ions as nodes and bridged ligands as spacers is still a major

---

*Corresponding author. Email: n-safari@cc.sbu.ac.ir

Journal of Coordination Chemistry
ISSN 0095-8972 print/ISSN 1029-0389 online © 2010 Taylor & Francis
DOI: 10.1080/00958972.2010.509794

challenge [4, 5]. Copper is an essential element, which plays a vital role in a number of quite different biological processes [6].

The key step for polymeric transition metal complexes is to select appropriate multi-dentate ligands. As spacers, terephthalic acid (H_2tpht) and its dianion have been used because they can be mono-, bi-, tri-, or tetra-dentate ligands leading to a variety of structures [7–10]. H_2tpht has been extensively studied in the field of molecular magnetism with promising applications to high-density magnetic recording [11].

More recently, π-accepting ligands such as bithiazole have been of interest because they stabilize a particular electronic configuration of the associated metal such as copper. This interaction generates metal–ligand excited transfer states which can be studied through their photoluminescence properties [12].

Bithiazole, one domain of bleomycin (BLM), was shown to be responsible for binding of BLM to DNA [13]. Copper complexes are widely used as footprint DNA binding molecules and cleaving reagents [14]. For instance, Ni and Co complexes of 2,2′-diamino-4,4′-bithiazole are effective inhibitors of DNA synthesis in tumor cells [15, 16] and Fe(II), Fe(III), and Cu(II) complexes have found application in soft magnetic materials [17–20].

Here, we report copper complexes of bithiazole and terephthalate (tpht). Most of the published works concern μ-tpht–copper complexes having *zigzag* chains with *anti*-configuration; we prepared the first μ-tpht–copper complex with 2,2′-dimethyl-4,4′-bithiazole (dm4bt) with *cis*-configuration.

2. Experimental

2.1. *Materials and instruments*

All chemicals were purchased from Merck. Infrared (IR) spectra (4000–250 cm^{-1}) of solid samples were taken as 1% dispersion in CsI pellets using a Shimadzu-470 spectrometer. UV-Vis spectra were recorded on a Shimadzu 2100 spectrometer using a 1 cm path length cell. X-band electron paramagnetic resonance (EPR) spectra were recorded on powder and frozen solutions at room and liquid nitrogen temperatures on an IBM electron spin resonance (ESR) spectrometer using 2,2-diphenyl-1-picrylhydrazyl (DPPH) ($g = 2.0036$) as a standard. Melting points are uncorrected, obtained by a Kofler Heizbank Rechart type 7841 melting point apparatus. Elemental analyses were performed using a Heraeus CHN–O Rapid analyzer.

2.2. *Synthesis of [Cu(dm4bt)Cl$_2$(DMSO)] (1)*

H_2tpht (0.04 g, 0.25 mmol) was dissolved in 1 mL methanol and 1 mL water, then solid $CuCl_2 \cdot 2H_2O$ (0.04 g, 0.25 mmol) was added to a solution and stirred for about 20 min. To this solution, dm4bt (0.05 g, 0.25 mmol) in 5 mL methanol was added, but the acid did not dissolve. During stirring of the pale green solution, drops of DMSO were added and the solution was stirred 45 min at 40–45°C. After 3 months, orange block crystals of **1** were isolated (yield 0.077 g, 75%, m.p. 243–245°C). IR (CsI, cm^{-1}): 3390br, 3101w, 3086s $\nu(C\text{–}H_{cycle})$, 2983w, 2923m, 2839w $\nu(C\text{–}H_{Me})$, 1657m $\nu(C{=}C)$, 1525m $\nu(C{=}N)$, 1437m ν(C–C), 1372m, 1289m, 1204s ν(C–N), 1157s, 1025m, 943m ν(S=O), 857w ν(S–C), 753s, 691m, 637w, 585w, 450w ν(Cu–O_{DMSO}), 352w, 332w ν(Cu–N), 299w ν(Cu–Cl). UV-Vis: λ_{max}: $3.75 \times 10^4\,cm^{-1}$. Anal. Calcd for $C_{10}H_{14}Cl_2CuN_2OS_3$ (%): C, 29.37; H, 3.42; and N, 6.85. Found: C, 29.24; H, 3.38; and N, 6.78.

2.3. *Synthesis of $[\{Cu(dm4bt)(H_2O)(tpht)\} \cdot H_2O]_n$ (2)*

H_2tpht (0.04 g, 0.25 mmol) was dissolved in 1 mL methanol, 1 mL water, and 1 mL ethylene diamine (0.30 mol L^{-1} in methanol solution). Then, solid $CuCl_2 \cdot 2H_2O$ (0.04 g, 0.25 mmol) was added to the solution and stirred for 30 min until a precipitate was formed. The precipitate started to disappear gradually when dm4bt (0.05 g, 0.25 mmol) was added to the solution, but did not disappear completely until 10 mL of water was added to the solution. The resulting violet solution was stirred at 40–45°C for 1 h. After 2 months, dark green crystals of **2** were isolated (yield 0.087 g, 76%, m.p. 230°C). IR (CsI, cm^{-1}): 3799w, 3745w, 3646w, 3622s, 3564w, 3461br ν(H_2O), 3225br, 3105m ν(C–H_{cycle}), 2923w ν(C–H_{Me}), 1700w ν(C=O), 1609s ν_{as}(COO), 1540m ν(C=C), 1501w ν(C=N), 1433m ν(C–C), 1364s ν_s(COO), 1296w, 1212m ν(C–N), 1170w, 1087w, 1042w, 1019w, 974w, 883w, 819m ν(S–C), 797m, 770m, 746s, 652w, 598w, 525m, 420w ν(Cu–O_w), 397w, 372w ν(Cu–O_{pht}), 352w ν(Cu–N), 279m. UV-Vis λ_{max}: $3.61 \times 10^4\,cm^{-1}$. Anal. Calcd for $C_{16}H_{16}Cu_1N_2O_6S_2$ (%): C, 41.78; H, 3.48; and N, 6.09. Found: C, 41.64; H, 3.42; and N, 5.98.

2.4. *Crystal structure determination and refinement*

X-ray diffraction measurements were made on a STOE IPDS-II diffractometer for **1** and Bruker Smart APEX diffractometer for **2** with graphite monochromated Mo-Kα radiation. For **1**, an orange block crystal ($0.50 \times 0.40 \times 0.15\,mm^3$) and for **2**, a dark green block crystal ($0.02 \times 0.04 \times 0.12\,mm^3$) were mounted on a glass fiber and used for data collection. The data were obtained by least-squares refinement of diffraction data from 3997 for **1** and 4552 for **2** unique reflections. Data were collected at 120(2) K to a maximum 2θ value of 58.4° for **1** in a series of ω scans in 1° oscillations and integrated using the Stoe X-AREA [21] software package. For **2**, the data were collected at a temperature of 123(2) K to a maximum 2θ value of 50° in a series of ω scans in 1° oscillations and integrated using the Stoe X-AREA [21] software package. The numerical absorption coefficient, μ, for Mo-Kα radiation is 2.209 mm^{-1} for **1** and 1.478 mm^{-1} for **2**. For **1**, a numerical absorption correction using X-RED [22] and X-SHAPE [23] softwares and for **2**, a multi-scan absorption correction using SADABS [24] was applied. The data were corrected for Lorentz and polarizing effects. The structures were solved by direct methods [24] and subsequent difference Fourier maps and then refined on F^2 by a full-matrix least-squares procedure using anisotropic displacement parameters [25]. All hydrogens were located in ideal positions and then refined isotropically. Atomic factors are from International Tables for X-ray Crystallography [26]. A summary of crystal data, experimental details, and refinement results are given in table 1.

Table 1. Crystallographic and structural refinement data for **1** and **2**.

	1	**2**
Empirical formula	$C_{10}H_{14}Cl_2CuN_2OS_3$	$C_{16}H_{16}CuN_2O_6S_2$
Formula weight	408.89	459.97
Temperature (K)	120(2)	123(2)
Wavelength (Å)	0.71073	0.71073
Crystal system	Monoclinic	Monoclinic
Space group	$P2(1)/c$	$P2(1)/c$
Unit cell dimensions (Å, °)		
a	9.8826(8)	8.698(3)
b	7.8621(4)	23.693(7)
c	19.6250(15)	19.065(3)
β	98.513(6)	104.868(7)
Volume (Å^3), Z	1508.02(18), 4	1805.66(10), 4
Calculated density (g cm^{-3})	1.801	1.682
Absorption coefficient (mm^{-1})	2.209	1.478
$F(000)$	828	940
Crystal size (mm^3)	$0.50 \times 0.40 \times 0.15$	$0.12 \times 0.04 \times 0.02$
θ ranges for data collection (°)	2.10–29.20	1.70–25.00
Limiting indices	$-9 \le h \le 13$; $-10 \le k \le 10$; $-26 \le l \le 26$	$-9 \le h \le 10$; $-28 \le k \le 28$; $-10 \le l \le 10$
Reflections collected	11,215	8480
Independent reflection	3997 [$R_{(int)} = 0.0601$]	3174 [$R_{(int)} = 0.0960$]
Parameters/restraints	172/0	246/6
Goodness-of-fit on F^2	1.062	0.960
Final R indices [$I > 2\sigma(I)$]	$R_1 = 0.0520$, $wR_2{}^a = 0.1447$	$R_1 = 0.0562$, $wR_2{}^a = 0.1079$
R indices (all data)	$R_1 = 0.0529$, $wR_2{}^a = 0.1459$	$R_1 = 0.1121$, $wR_2{}^a = 0.1338$
Largest difference peak and hole (e Å^{-3})	1.531 and −1.574	0.480 and −0.526

[a] $R_1 = \Sigma||F_o| - |F_c||/\Sigma|F_o|$, $wR_2 = [\Sigma(w(F_o^2 - F_c^2)^2)/\Sigma w(F_o^2)^2]^{1/2}$.

3. Results and discussion

3.1. *Synthesis of 1 and 2*

Compound **1** was obtained from the reaction of one equivalent of $CuCl_2 \cdot 2H_2O$ with one equivalent of dm4bt and one equivalent terephthalic (1,4-benzenedicarboxylic) acid, H_2tpht, in a mixture of methanol, water, and DMSO at 40–45°C during 45 min in 75% yield. Compound **2** was obtained from the reaction of one equivalent of $CuCl_2 \cdot 2H_2O$ with one equivalent of dm4bt, one equivalent of H_2tpht, and one equivalent ethylene diamine in a mixture of methanol and water at 40–45°C during 1 h in 76% yield. H_2tpht is not coordinated in **1** and the presence of a base is required to replace the chlorides by tpht as seen in **2** (scheme 1). Other tphts coordinated to Cu(II) complexes are also reported in the presence of bases, such as Na_2CO_3 [8] and NaOH [27].

We have previously reported the synthesis and crystal structure of dm4bt and also its zinc, mercury, cadmium, thallium, and copper complexes resulting from $ZnCl_2$, $HgCl_2$, $CdCl_2$, $Cd(NO_3)_2 \cdot 4H_2O$, $Tl(NO_3)_3 \cdot 3H_2O$, $CuCl_2 \cdot 2H_2O$, and $Cu(NO_3)_2 \cdot 3H_2O$ [28–31]. In all of these cases, we obtained monomeric compounds with [Zn(dm4bt)Cl_2], and [{Cu(dm4bt)$_2$(NO_3)}NO_3]. Dimeric compounds in which one of the two chlorides is set at a semi-bridging position were formed with [M(dm4bt)Cl_2]$_2$, where M = Hg and Cu [28, 31]. We have also synthesized a 1-D *zigzag*

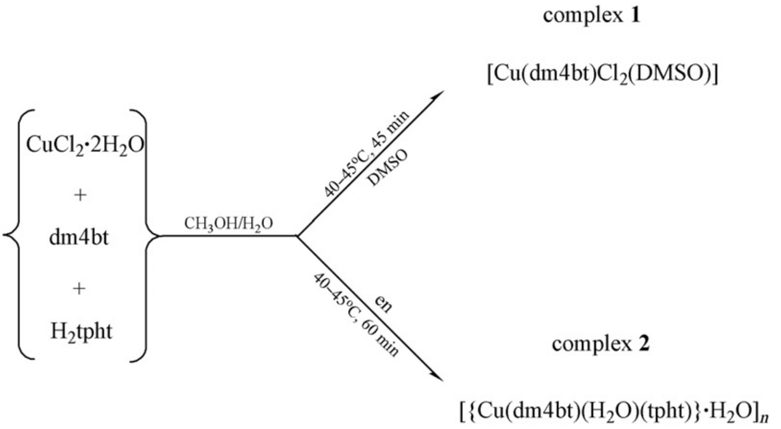

Scheme 1. The preparation method of complexes **1** and **2**.

Table 2. Selected IR frequencies (cm^{-1}) for **1** and **2**.

	dm4bt	H$_2$tpht	DMSO	**1**	**2**
ν(C–H)cycle	3450, 3124, 3043	3060, 3006	–	3390, 3101, 3086	3225, 3105
ν(C–H)Me	3017	–	2913, 2996	2983, 2839	2923
ν(C=C)	1541	1582	–	1657	1540
ν(C=N)	1507	–	–	1525	1501
ν(C–C)	1443	1452	–	1437	1433
ν(C–N)	1158	–	–	1204	1212
ν(S–C)	881	–	753	857	883
ν(S=O)	–	–	1050	943	–
ν(Cu–N)	–	–	–	352	352
ν(Cu–Cl)$_{\text{terminal}}$	–	–	–	299	–
ν(Cu–O)$_{\text{DMSO}}$	–	–	–	450	–
ν_{as}(COO)	–	–	–	–	1609
ν_{s}(COO)	–	–	–	–	1364
ν(C=O)	–	–	–	–	1700
ν(O–H$_2$)	–	–	–	–	3461
ν(Cu–O$_{\text{pht}}$)	–	–	–	–	372
ν(Cu–O$_{\text{W}}$)	–	–	–	–	420

coordination polymer which contains bridging chlorides [Cd(dm4bt)Cl$_2$]$_n$ from cadmium(II) chloride [29].

3.2. *IR and UV-Vis investigation*

Infrared spectra for dm4bt, **1** and **2**, presented in table 2, contain several bands in the region 800–3400 cm^{-1}, which are related to the heteroaromatic ring modes related to C–H, C=C, C=N, C–C, C–N, and S–C [32]. For instance, bands observed at 1541, 1507, 1471, 1443, 1261, 1158, 881, and 782 cm^{-1} for the free ligand are shifted to higher frequencies upon coordination (1657, 1525, 1437, 1204, 1157, 857, and 787 cm^{-1} in **1**). This shift to higher frequencies upon coordination to metal has been observed for bipyridine and other ligands as well [33–36], arising from changing the geometry of the free ligand from *syn* to *anti* upon coordination. The same trend was observed for **2**. The IR spectra of **1** and **2** are distinguished from that of dm4bt mainly by the metal-to-ligand bands. Strong peaks at 352 cm^{-1} were assigned to ν(Cu–$N_{thiazol}$) for **1** and **2** [34]. The band at 299 cm^{-1} was assigned to ν(Cu–Cl) in **1** [37–39] and the band at 450 cm^{-1} was assigned to ν(Cu–O_{DMSO}). Bands at 420 and 372 cm^{-1} were assigned to ν(Cu–O_w) and ν(Cu–O_{pht}), respectively, in **2** [39].

The IR spectrum of **2** shows the coordination of tpht; strong bands correspond to ν_{as}(COO) at 1609 cm^{-1} and ν_s(COO) at 1364 cm^{-1} [39]. The $\Delta\nu$ value of 245 cm^{-1} agrees with monodentate carboxylate [4, 40]. In addition, in **2**, the broad absorption band at 3461 cm^{-1} and sharp band at 3622 cm^{-1} are assigned for ν(O–H) of coordinated and lattice water [27, 40].

Electronic spectra were taken in the 900–200 nm range in DMSO for both complexes. The intense band at $3.75 \times 10^4\,cm^{-1}$ for **1** and $3.60 \times 10^4\,cm^{-1}$ for **2** are in agreement with intra-ligand π–π* transitions of bithiazole which is at $3.85 \times 10^4\,cm^{-1}$. The visible region also contains very low intensity absorbance at $1.29 \times 10^4\,cm^{-1}$ for **1** and $2.50 \times 10^4\,cm^{-1}$ for **2** which are assigned to d_{xy}, $d_{yz} \rightarrow d_{x^2-y^2}$ transition [41].

3.3. *EPR investigation of 2*

The X-band EPR spectra of **2** were measured at room temperature in polycrystalline state and at liquid nitrogen temperature in solution, as shown in "Supplementary material." It exhibits an asymmetrical signal at room temperature which slightly resolves at liquid nitrogen temperature. The $g_{\parallel}$ value (2.30) is higher than that of $g_{\perp}$ (2.06), indicating a non-degenerate $d_{x^2-y^2}$ ground state [42]. In addition, $G = (g_{\parallel}-2)/(g_{\perp}-2)$ for polycrystalline and solution glass are 4.56 and 5.00, respectively, which indicates $d_{x^2-y^2}$ ground state [43]. The unpaired electron in the $d_{x^2-y^2}$ orbital produces a characteristic $S = ½$ signal with $g_{\parallel} > g_{\perp} > 2.0023$. The naturally occurring isotopes ^{63}Cu and ^{65}Cu (abundance 69% and 31%, respectively) have a nuclear spin of 3/2 which couples to the electron spin to produce a $2I + 1$ or four line hyperfine splitting of the EPR signal [44]. The parallel hyperfine splitting, $A_{\parallel}$, observed for normal tetragonal copper(II) complexes is generally in the range 150×10^{-4}–$250 \times 10^{-4}\,cm^{-1}$. The hyperfine splitting in the $g_{\parallel}$ region, $A_{\parallel} = 54 \times 10^{-4}\,cm^{-1}$ for solid state at room temperature and for solution glass (liquid nitrogen temperature). Thus, we believe the complex has similar structures in both conditions. The $A_{N\perp}$ of $5 \times 10^{-4}\,cm^{-1}$ and the presence of five peaks for the nitrogen superhyperfine structure for the complex agrees with two *N* donors to copper(II) [45, 46].

3.4. *Description of the molecular structure of 1 and 2*

Selected bond lengths and angles for **1** and **2** are listed in table 3. The atomic numbering scheme and atom connectivity for **1** is shown in figure 1. In this compound, Cu(II) has a slightly distorted square pyramidal geometry, with trigonality index $\tau = 0.14$ ($\tau = (\beta - \alpha)/60$, where β is the greatest basal angle and α the second in magnitude; $\tau = 0$ and 1 for perfect square pyramidal and trigonal bipyramidal geometries, respectively) [47]. In this structure, the basal plane is made up of two thiazoline nitrogens N(1) and N(2), one DMSO oxygen O(1) and Cl(2), and the apical site is occupied by the other chloride Cl(1). According to their distances and angles from copper;

Table 3. Selected bond distances (Å) and angles (°) for **1** and **2**.

1			
Cu(1)–O(1)	2.017(2)	N(1)–Cu(1)–Cl(2)	159.69(8)
Cu(1)–N(1)	2.046(2)	N(2)–Cu(1)–Cl(2)	94.93(7)
Cu(1)–N(2)	2.057(2)	N(1)–Cu(1)–Cl(1)	99.14(6)
Cu(1)–Cl(1)	2.482(7)	N(2)–Cu(1)–Cl(1)	106.45(3)
Cu(1)–Cl(2)	2.276(8)	Cl(2)–Cu(1)–Cl(1)	102.45(3)
O(1)–Cu(1)–Cl(1)	100.48(7)	N(1)–Cu(1)–O(1)	86.84(9)
O(1)–Cu(1)–Cl(2)	88.88(6)	N(2)–Cu(1)–O(1)	151.46(9)
2			
Cu(1)–O(1)	1.979(4)	N(1)–Cu(1)–N(2)	78.26(19)
Cu(1)–O(3)^{i}	1.945(4)	N(1)–Cu(1)–O(1)	95.27(17)
Cu(1)–O(1)W	1.966(4)	N(2)–Cu(1)–O(1)	89.54(18)
Cu(1)–O(2)	2.890(5)	N(1)–Cu(1)–O(2)	145.47(15)
Cu(1)–N(1)	2.265(5)	N(2)–Cu(1)–O(2)	94.38(17)
Cu(1)–N(2)	2.034(5)	N(1)–Cu(1)–O(1)W	99.90(18)
O(1)–Cu(1)–O(3)^{i}	173.40(17)	N(2)–Cu(1)–O(1)W	178.02(19)
O(1)–Cu(1)–O(1)W	89.93(17)	N(1)–Cu(1)–O(3)^{i}	91.29(18)
O(3)^{i}–Cu(1)–O(1)W	88.27(17)	N(2)–Cu(1)–O(3)^{i}	92.47(18)

Symmetry transformations used to generate equivalent atoms: $^{i}x+1$, y, $z+1$.

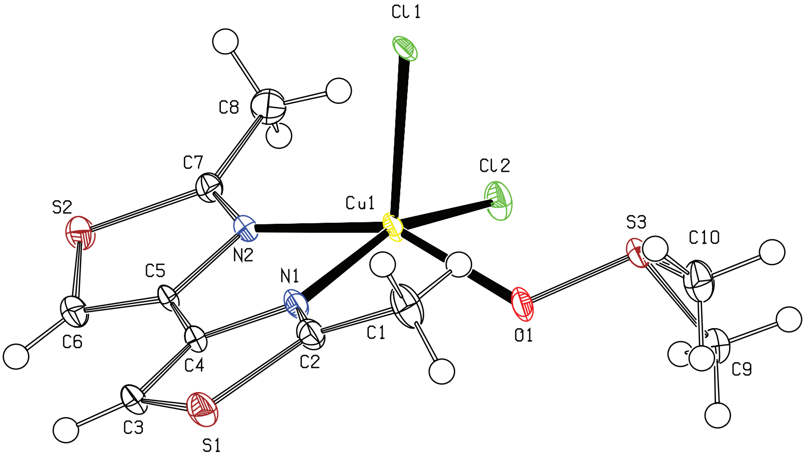

Figure 1. Graphical representation of **1** (50% probability for the thermal ellipsoids).

Cl(2)–Cu(1)–Cl(1) ~ 102.5°, N(2)–Cu(1)–Cl(1) ~ 106.5°, and O(1)–Cu(1)–Cl(1) ~ 100.5°, this structure is described as a slightly distorted square pyramid. Square pyramidal geometry is distorted with Cl(1) in axial position and elongated due to Jahn–Teller distortion. Furthermore, a single guest of DMSO disordered this geometry, where Cu(1)–O(1)–S(3) ~ 118.7° with sulfur disordered as well. As shown in figure 2, in **1**, the thiazole rings form π bonding stacks in the *b*-direction. The close contact distance between adjacent aromatic rings is 3.48 Å. In addition, there are S ··· Cl interactions in the *a*-direction.

The structure of **2** is isostructural to the previously reported complexes with the general formula [M(tpht)(phen)(H_2O)]$_n$ (where tpht = terephthalate, phen = 1,10-phenanthroline, and M = Co(II), Zn(II), and Cu(II)) [9, 48]. In addition, the structures of the similar [M(tpht)(phen)]$_n$ (M = Mn(II) and Cu(II)) and [Cd(tpht)(phen)Cl]$_n$

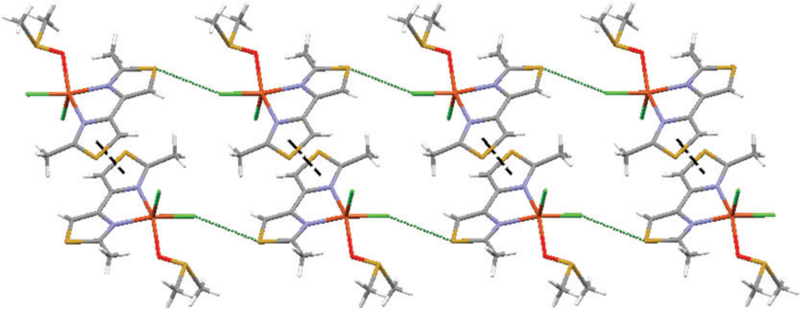

Figure 2. The unit cell packing diagram of **1**. The π–π interactions between thiazole rings and the S···Cl interactions are shown as dashed lines.

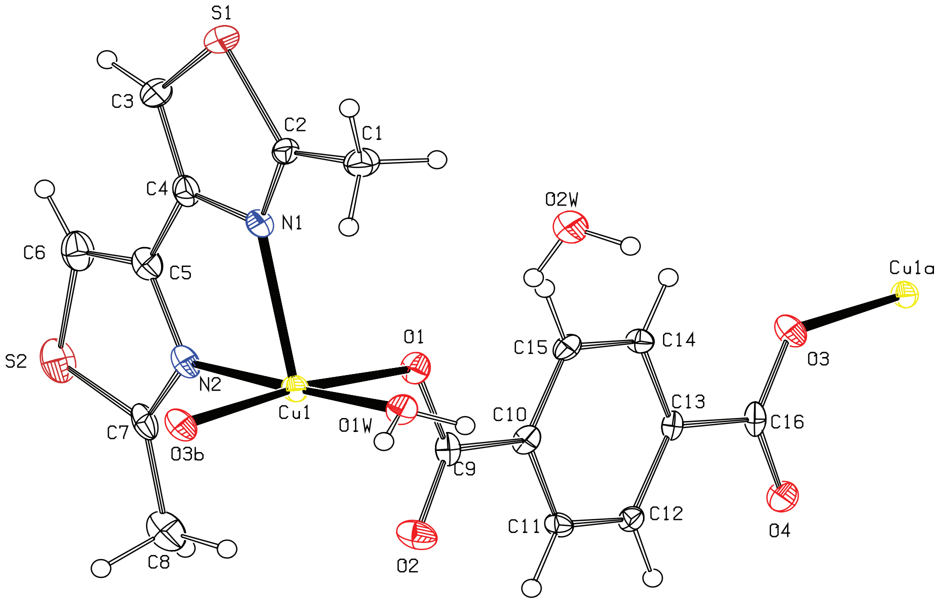

Figure 3. Graphical representation of **2** (30% probability for the thermal ellipsoids). Symmetry codes: a: $-1+x$, y, $-1+z$ and b: $1+x$, y, $1+z$.

containing the same ligands are known [48]. Since the crystallographic center coincides with the centers of both aromatic rings of dm4tb, as shown in figure 3, only half of each tpht belongs to the asymmetric unit. The dm4bt is a chelate with typical Cu–N distances and a characteristic N–Cu–N chelating angle (table 3).

The tpht ligands are monodentate with Cu(1)–O(1) and Cu(1)–O(3) distances of 1.980 and 1.945 Å, respectively. Therefore, each tpht is a bridging ligand linking two metal centers and each metal center coordinates two tpht ligands to form a 1-D linear chain. The neighboring dm4bt ligands are *cis* to each other (figure 4). This linear chain is different than reported *zigzag* chains with *anti*-configuration for [M(tpht)(phen)$(H_2O)]_n$ (M = Co(II), Zn(II), and Cu(II)), $[M(tpht)(phen)]_n$ (M = Mn(II) and Cu(II)) [9, 48], [{$Cd_2(tpht)_2$((*E*)-N^1,N^1-diethyl-N^2-(1-(pyridin-2-yl)ethylidene)ethane-1,2-diamine)$_2$} $\cdot$ $9H_2O$] [49], [Cu(4,4-dimethylbipyridine)$(N_3)]_2$(tpht)$2CH_3OH \cdot 2H_2O$ [50],

Table 4. Geometry of the hydrogen bonds (Å) of **2**.

D–H···A	*d*(D–H) (Å)	*d*(H···A) (Å)	*d*(D···A) (Å)	(D–H···A) (°)
O1W–H11···O2^{iii}	0.8400	1.8200	2.651(6)	169.00
O1W–H12···O4^{iv}	0.8400	1.8600	2.684(6)	167.00
O2W–H21···O1	0.8400	2.0500	2.866(6)	163.00
O2W–H22···O4^{v}	0.8400	2.2600	3.031(6)	154.00
C3–H3···O2W	0.9500	2.3000	3.237(8)	168.00
C6–H6···O2W	0.9500	2.4800	3.389(8)	161.00
C8–H8A···O2	0.9800	2.3700	3.228(8)	146.00

Symmetry codes: $^{iii}-x+1, -y+1, -z+1$; $^{iv}-x, -y, -z$; $^{v}x+1, y, z$.

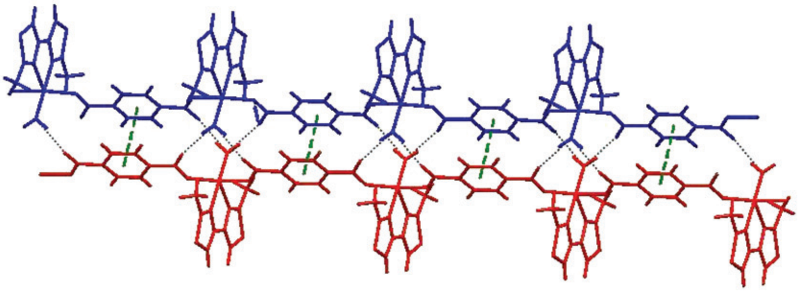

Figure 4. The unit cell packing diagram of **2**. The π–π interactions between tpht rings and hydrogen bonds are shown as dashed lines.

and [Cu(tpht)(4,7-dimethylphen)]$_n\cdot 0.5(H_2$tpht) [51], even with tridentate *N*-donor ligands, such as [{Cu$_2$(tpht)$_2$(tris(pyrazolyl)methane)$_2$} $\cdot$ H$_2$O]$_n$ [4], or with tetradentate *N*-donor ligands, such as [Ni(1,4,7,10-tetraazacyclododecane)(H$_2$O)$_2$](tpht) [52]. Thus, we believe that dm4bt has less steric hindrance than other chelating bidentate terminal/base ligands, such as phen. To the best of our knowledge, **2** with dm4bt in *cis*-configuration is the first reported one.

The plane of dm4bt is perpendicular to the aromatic rings of tpht. Usual for such compounds [4, 11, 40], Cu–O$_{\text{tpht}}$ distances (table 3) are significantly shorter than Cu–N$_{\text{thizo}}$ groups; this could be a consequence of the very short and strong Cu–O bond that increases the O–C bond order toward double bond character. In addition, copper formed monodentate and short bridges *via* one carboxylate. Since the maximum coordination number of copper is 6, tpht is prevented from bidentate coordination.

Complex **2** has a highly distorted square pyramidal geometry, with trigonality index $\tau = 0.36$. The atomic numbering scheme and atom connectivity are shown in figure 3. According to the bond distances and the angles, the basal plane consists of three oxygens O(1), O(3)^{i}, and O(1)W and one nitrogen N(2), while the apical site is occupied by N(1), due to the Jahn–Teller distortion in the *z*-direction (2.3 *vs*. 2.0 Å) and the two nitrogens of chelating bithiazole ligand (with N(1)–Cu(1)–N(2) ~ 78.25°). The geometry appeared as a distorted square pyramid.

There are two kinds of water molecules in this complex, one coordinated and the other free. The coordinated H$_2$O molecule is a double H–bonding donor toward O(2) and O(4) from COO groups, which belongs to a parallel chain (figure 4). Moderately strong intermolecular hydrogen bonds (O1–H11···O2) and (O1–H12···O4), table 4, may be envisaged between the non-coordinated oxygens of the carboxylic groups and the coordinated water molecule. While the free water stays between the 1-D linear chains, this molecule works as a spider net which tries to hold the linear chains as parallel layers. Moreover, π–π interactions formed between these parallel chains. Overall, the tphts are coligand *via* the deprotonated carboxylate groups to build coordination networks as well as interlink the 1-D chains into frameworks *via* hydrogen bonds and π–π interactions, as shown in figure 4.

Therefore, infinite 1-D chains running along the *c*-axis are formed, as depicted in figure 4, with $Cu\cdots Cu$ distances along the linear chain around 10.834 Å. The $Cu\cdots Cu$ interaction through space between parallel chains is around 4.901 Å. Indeed, these $Cu\cdots Cu$ interaction distances are in harmony with the values recorded in the literature and fit quite well for tpht bridges [9, 40, 50].

Furthermore, these interactions increase the stability of the crystal lattice and insolubility of **2**.

4. Conclusion

Two new copper(II) complexes were synthesized and their structures were characterized by X-ray crystallography and spectroscopic methods. Investigation was performed to make H_2tpht a bridging ligand with copper(II) chloride dihydrate and dm4bt. First, we followed the literature procedure to deprotonate H_2tpht by using a mixture of methanol, water, and DMSO, but our attempt was not successful. We then used a mixture of methanol, water, and diamine as a new way to deprotonate this acid. Thus, polymeric **2** was formed as a new complex, although in the former attempt an interesting monomeric compound, **1**, was formed.

Supplementary material

CCDC nos 752991 and 752990 contain the supplementary crystallographic data for **1** and **2**, respectively. These data can be obtained free of charge *via* http://www.ccdc.cam.ac.uk/conts/retrieving.html, or from the Cambridge Crystallographic Data Centre, 12 Union Road, Cambridge CB2 1EZ, UK. Fax: +44-1223-3360033; Email: deposit@ccdc.cam.ac.uk.

Acknowledgments

We thank the Graduate Study Councils of the Shahid Beheshti University for the financial support (Project 600/1207).

References

[1] H.J. Chen, J. Zhang, W.L. Feng, M. Fu. *Inorg. Chem. Commun.*, **9**, 300 (2006).

[2] S.G. Baca, S.T. Malinovskii, P. Franz, C. Ambrus, H. Stoeckli-Evans, N. Gerbeleu, S. Decurtins. *J. Solid State Chem.*, **177**, 2841 (2004).
[3] F.Q. Liu, Q.X. Wang, K. Jiao, F.F. Jian, G.Y. Liu, R.X. Li. *Inorg. Chim. Acta*, **359**, 1524 (2006).
[4] B. Zhai, W.Z. Shen, X.Y. Chen, H.B. Song, W. Shi, P. Cheng. *Inorg. Chem. Commun.*, **9**, 1293 (2006).
[5] Y.H. Wen, J.K. Cheng, Y.L. Feng, J. Zhang, Z.J. Li, Y.G. Yao. *Inorg. Chim. Acta*, **358**, 3347 (2005).
[6] J. Moncol, M. Korabik, P. Segl'a, M. Koman, D. Mikloš, J. Jašková, T. Glowiak, M. Melník, J. Mrozinski, M.R. Sundberg. *Z. Anorg. Allg. Chem.*, **633**, 298 (2007).
[7] S.P. Xu, C.H. Liu, C.H. Zhu. *Z. Kristallogr. NCS.*, **221**, 1 (2006).
[8] D.D. Lin, D.J. Xu. *J. Coord. Chem.*, **58**, 605 (2005).
[9] J. Rogan, D. Poleti, L. Karanovic. *J. Serb. Chem. Soc.*, **69**, 353 (2004).
[10] Q. Meng, L. Wang, Y. Liu, Y. Pang. *Acta Crystallogr.*, **E64**, m133 (2008).
[11] P.Y. Bu, L.Z. Zhang, L.C. Li, P. Cheng, S.P. Yan, Z.H. Jiang, D.Z. Liao. *J. Chem. Crystallogr.*, **33**, 257 (2003).
[12] N.B. Cherif, M. Pierrot. *Acta Crystallogr.*, **C51**, 72 (1995).
[13] S. Dhar, M. Nethaji, A.R. Chakravarty. *Dalton Trans.*, 4180 (2004).
[14] H. Sasaki, S. Takanori, K. Yamamoto, Y. Nakamoto. *Chem. Pharm. Bull.*, **44**, 1761 (1996).
[15] Y. Tian, P. Yang, Q. Li, S. Liu. *J. Coord. Chem.*, **41**, 223 (1997).
[16] Y. Tian, P. Yang, H.F. Wang, Y.L. Feng, S.X. Liu, J.L. Huang. *Polyhedron*, **15**, 2771 (1996).
[17] W. Sun, X. Gao, F. Lu. *J. Appl. Polym. Sci.*, **64**, 2309 (1997).
[18] J. Weng, W. Sun, L. Jiang, Z. Shen. *Macromol. Rapid Commun.*, **21**, 1099 (2000).
[19] L. Jiang, W. Sun. *Polym. Adv. Technol.*, **16**, 646 (2005).
[20] C. Janiak, L. Uhelin, H. Wu, P. Klufers, H.G. Piotrowski, T. Scharmann. *J. Chem. Soc., Dalton Trans.*, 3121 (1999).
[21] Stoe & Cie. *X-AREA*, *Program for the Acquisition and Analysis of Data*, (*version* 1.30), Stoe & Cie GmbH, Darmstadt, Germany (2005).
[22] Stoe & Cie. *X-RED*, *Program for Data Reduction and Absorption Correction*, (*version* 1.28b), Stoe & Cie GmbH, Darmstadt, Germany (2005).
[23] Stoe & Cie. *X-SHAPE*, *Program for Crystal Optimization for Numerical Absorption Correction*, (*version* 2.05), Stoe & Cie GmbH, Darmstadt, Germany (2004).
[24] G.M. Sheldrick. *SADABS*, University of Göttingen, Germany (1996).
[25] G.M. Sheldrick. *Acta Crystallogr.*, **A64**, 112 (2008).
[26] E. Prince (Ed.), *International Tables For X-ray Crystallography*, Vol. C, Table 6.1.1.4, pp. 577–580, Kluwer Academic Publisher, Doordrecht, Netherlands (2004).
[27] A. Company, L. Gómez, J.M.L. Valbuena, R. Mas-Ballestè, J. Benet-Buchholz, A. Llobet, M. Costas. *Inorg. Chem.*, **45**, 2501 (2006).
[28] H.R. Khavasi, A. Abedi, V. Amani, B. Notash, N. Safari. *Polyhedron*, **27**, 1848 (2008).
[29] B. Notash, N. Safari, A. Abedi, V. Amani, H.R. Khavasi. *J. Coord. Chem.*, **62**, 1638 (2009).
[30] B. Notash, N. Safari, H.R. Khavasi, V. Amani, A. Abedi. *J. Organomet. Chem.*, **693**, 3553 (2008).
[31] R. Al-Hashemi, N. Safaria, A. Abedi, B. Notash, V. Amani, H.R. Khavasi. *J. Coord. Chem.*, **62**, 2909 (2009).
[32] M.G. Drew, T.R. Pearson, B.P. Murphy, S.M. Nelson. *Polyhedron*, **2**, 269 (1983).
[33] A. Neels, H.S. Evans. *Inorg. Chem.*, **38**, 6164 (1999).
[34] L. Jiang, W. Sun, J. Weng, Z. Shen. *Polymer*, **43**, 1563 (2002).
[35] A.K. Boudalis, C.P. Raptopoulou, A. Terzis, S.P. Perlepes. *Polyhedron*, **23**, 1271 (2004).
[36] V. Amani, N. Safari, H.R. Khavasi. *Polyhedron*, **26**, 4257 (2007).
[37] J.A. Weaver, P. Hambright, P.T. Talbert, E. Kang, A.N. Thorpe. *Inorg. Chem.*, **9**, 268 (1970).
[38] F.J.B. García, A.B. García, F.J.H. Rolando, F.L. Giles, A.M.P. Galán, E.V. Zahínos. *Z. Anorg. Allg. Chem.*, **631**, 1898 (2005).
[39] K. Nakamoto. *Infrared and Raman Spectra of Inorganic and Coordination Compounds Part B: Applications in Coordination, Organometallic, and Bioinorganic Chemistry*, 5th Edn, John Wiley & Sons, New York (1997).
[40] Y.T. Li, Z.Q. Liu, Z.Y. Wu. *J. Inorg. Biochem.*, **102**, 1790 (2008).
[41] Y.Y. Wang, L.J. Zhou, Q. Shi, Q.Z. Shi. *Transition Met. Chem.*, **27**, 145 (2002).
[42] M. Du, Y.M. Guo, X.H. Bu. *Inorg. Chim. Acta*, **335**, 136 (2002).
[43] E.I. Solomon, U.M. Sundaram, T.E. Machonkin. *Chem. Rev.*, **96**, 2563 (1996).
[44] B.J. Hathaway, A.A.G. Tomlinson. *Coord. Chem. Rev.*, **5**, 1 (1970).
[45] A.L. Abuhijleh, C. Woods. *Inorg. Chim. Acta*, **209**, 187 (1993).
[46] H. Zheng, L. Que Jr. *Inorg. Chim. Acta*, **263**, 301 (1997).
[47] A.W. Addison, T.N. Rao, J. Reedjik, J.V. Rijn, G.C. Verschorr. *J. Chem. Soc., Dalton Trans.*, 1349 (1984).
[48] D. Sun, R. Cao, Y. Liang, Q. Shi, W. Su, M. Hong. *J. Chem. Soc., Dalton Trans.*, 2335 (2001).
[49] S. Banerjee, P.-G. Lassahn, C. Janiak, A. Ghosh. *Polyhedron*, **24**, 2963 (2005).
[50] L. Li, D. Liao, Z. Jiang, S. Yan. *J. Mol. Struct.*, **597**, 157 (2001).
[51] Y.H. Wen, S.W. Ng. *Acta Crystallogr.*, **E63**, m1865 (2007).
[52] Y.W. Ren, J. Li, S.M. Zhao, F.X. Zhang. *J. Struct. Chem.*, **16**, 439 (2005).